Journal of Radiotherapy in Practice

cambridge.org/jrp

Original Article

Cite this article: Kititharakun P, Nobnop W, Kongsa A, Thongsuk W, and Watcharawipha A. (2025) Surrounding dose investigation of real-time motion tracking system in tomotherapy. *Journal of Radiotherapy in Practice*. **24**(e42), 1–9. doi: 10.1017/S1460396925100290

Received: 1 September 2025 Revised: 3 November 2025 Accepted: 4 November 2025

Keywords:

Stereotactic ablative body radiotherapy; Gamma passing rate; real-time motion tracking; tomotherapy; surrounding dose area

Corresponding author:

Anirut Watcharawipha; Email: anirut.watch@cmu.ac.th

© The Author(s), 2025. Published by Cambridge University Press. This is an Open Access article, distributed under the terms of the Creative Commons Attribution licence (https://creativecommons.org/licenses/by/4.0/), which permits unrestricted re-use, distribution and reproduction, provided the original article is properly cited.



Surrounding dose investigation of real-time motion tracking system in tomotherapy

Phairot Kititharakun^{1,2}, Wannapha Nobnop², Anupong Kongsa², Warit Thongsuk² and Anirut Watcharawipha² (D

¹Medical physics program, Faculty of Medicine, Chiang Mai University, Chiang Mai, Thailand and ²Division of Radiation Oncology, Department of Radiology, Faculty of Medicine, Chiang Mai University, Chiang Mai, Thailand

Abstract

Purpose: This study investigated the dose difference (DD) in the surrounding dose area using the real-time motion tracking (RTMT) system in tomotherapy.

Method: Seven stereotactic ablative body radiotherapy treatment plans with a single lesion were used for the investigations. Each treatment plan was evaluated for the Gamma passing rate (GPR) analysis in a static target motion using the ArcCHECK* phantom. Subsequently, each plan was matched with 8 clinical respiratory cycles to simulate moving target motion. The DD was calculated through point-to-point comparison and expressed as the frequency of the DD levels. The DD frequency was analysed for significant correlations with the target travelling distance, target size and respiratory frequency.

Result: The GPR for criteria of 3%/2mm and 3%/3mm revealed values of $97.8 \pm 1.9\%$ and $99.5 \pm 0.6\%$, respectively, for static motion. The highest frequency of DD was in the 5-10% range. A significant correlation was found between the target travelling distance and the frequency of percent DD at the 2.0-3.0% and 10.0-15.0% levels, as well as between target size and the frequency of percent DD at the 0.0-4.0% and 10.0-25.0% levels. Finally, no significant correlation was found between the frequency of percent DD and respiratory frequency. Conclusion: RTMT introduced the DD in the surrounding treatment area. The DD was found to be up to 15.0% at 119.5 mm (water-equivalent distance) from the phantom centre. The DD was varied depending on the target travelling distance and size, but it did not depend on the respiratory frequency.

Introduction

Radiotherapy treatment techniques have been highly developed to maximize the benefits of cancer treatment. The main goal of curative treatment is to control the disease and reduce the complications to organs at risk (OARs), especially in stereotactic radiosurgery (SRS) or stereotactic ablative radiotherapy (SABR) (also known as stereotactic body radiotherapy, SBRT). High-precision treatment techniques are such as intensity-modulated radiation therapy^{1,2} (IMRT), volumetric-modulated arc therapy²⁻⁴ (VMAT), helical tomotherapy⁴⁻⁶ (HT), CyberKnife*⁷⁻⁹ and so forth.

Due to the requirement for high precision and accuracy in SRS/SABR, it is essential to keep the target as stable as possible. External immobilization devices are used for motion fixation, but internal organ motion cannot be controlled voluntarily. Therefore, the American Association of Physicists in Medicine (AAPM) released the report number 91¹⁰ on motion management in the respiratory system. Real-time motion tracking (RTMT) is an advanced motion management process that has been installed in some treatment machines such as HT and CyberKnife®. This system adjusts the beam direction to track the target motion during radiation delivery, ensuring the accuracy of target tracking and dose delivery, as confirmed by several publications. 11-13 Although the RTMT treatment technique provided the benefits of target dose escalation and minimized the normal tissue dose at the treatment area. 10,14 An issue of the dose in surrounding area may receive a dose different from the treatment planning because of the target motion. During the target irradiated treatment tracking, the normal tissue in the surrounding area may not have a motion corresponding to the target. This area could receive the radiation dose by sweeping the radiation beam. Therefore, Ferris et al. investigated the normal organ dose by using the RTMT treatment technique.¹⁵ They found the dose difference (DD) at the surrounding organ up to 39·1% for the heart. However, the study utilized the feasibility of the deformable image registration in 4-dimensional computed tomography (4DCT) for the DD observation. Moreover, the motions of the target were simulated. This could not be represented in the clinical respiratory cycle.

Measuring the surrounding dose often requires experimental verification of the DD between static and moving beam delivery. Dose measurement using film is a common method for planar

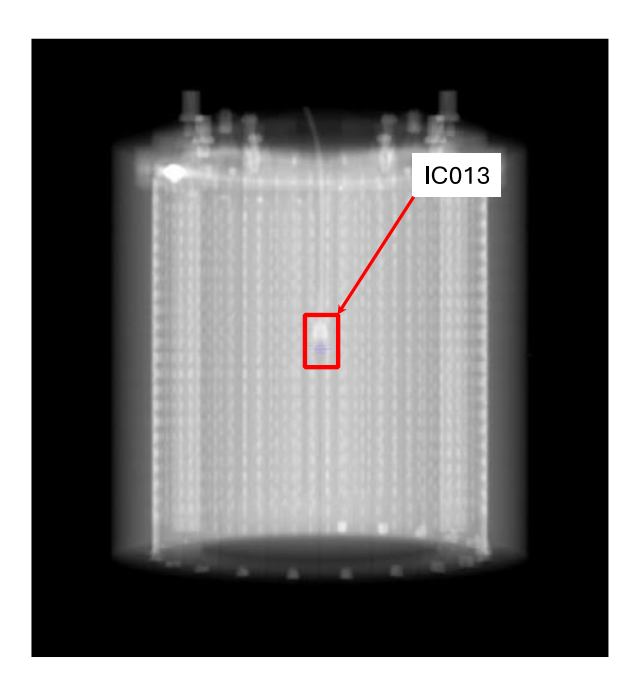


Figure 1. Position of ionization chamber 0.13 cc.

dose measurement, 16,17 but its uncertainty can increase, 18,19 particularly at low radiation doses. Two-dimensional array detectors may offer a more advantageous approach for dose measurement in this context. 20–22 Given the need to measure the surrounding dose, the detector's position is critical. A helical array detector may thus be suitable for this task. This study then investigated the surrounding dose area using two-dimensional helical array detectors placed on the near surface of the phantom. The study utilized the clinical respiratory motion for the target driven by a one-dimensional dynamic platform. The DD was compared between static target motion and moving target motion and expressed as the frequency of percent DD levels. Finally, the correlation was analysed using statistical correlation analysis between the frequency of percent DD levels and treatment characteristics.

Materials and Methods

Ethical clearance

This retrospective study enrolled SABR treatment plans with a single lesion of lung cancer. Seven treatment plans were randomly selected from the clinical treatment planning data of patients treated between January and December 2024. Additional treatment information, clinical respiratory cycles, was randomly obtained from a patient requiring thoracic treatment between January and February 2025. This study protocol was approved by the Research Ethics Committee of Faculty of Medicine, Chiang Mai University (Study code: RAD-2567-0221).

Patient-specific quality assurance treatment planning preparation

The selected treatment plans of seven patients were generated using the treatment plan of patient-specific quality assurance (PSQA). The computed tomography (CT) image set of ArcCHECK* (Sun Nuclear Co., FL, USA) was acquired by a CT simulator (SOMATOM Definition AS, Siemens Inc., Healthineers,

Germany) with a 1 mm slice thickness, and the PSQA plan was conducted. At the phantom centroid, the 0·13 cm³ ionization chamber (CC013, Scanditronix Wellhofer Inc., MN, USA) was inserted for the image registration and tracking marker when performing the dose delivery, as demonstrated in Figure 1. Although the lesion was in the peripheral lung, the geometry of the PSQA plan was set with this lesion at the phantom centroid. The calculated dose was performed in the highest resolution using the Precision® treatment planning system version 3.3.1.3 (Accuray Inc., Sunnyvale, CA, USA).

Respiratory cycle acquisition

The clinical respiratory cycle was randomly collected from patients who required treatment in the thoracic region. A single camera of surface-guided radiotherapy (SentinelTM, C-RAD AB, Sweden) was used to record the breathing cycle during the CT simulation. The surrogate point was placed at the xiphoid to observe the respiratory behaviour. The waveforms within the Synchronye criteria²³ were selected for this experiment. These waveforms were converted from CSV format to TXT format using MATLABe version R2021b (MathWorks Inc., MA, USA). This study then selected 8 out of 15 waveforms to match the PSQA treatment plan for the surrounding dose investigation. The frequency of the selected waveform samples was distributed in slightly equivalent intervals and demonstrated in Figure 2.

Dose difference at the surrounding area measurement setup

The surrounding dose measurement was conducted under two conditions using the Radixact* X9 with Synchrony* system (Accuray* Inc., Sunnyvale, CA, USA). All detectors of phantom measured the dose in static and moving target motion. The Gamma passing rate (GPR) was compared between the calculated dose and the measured dose using the 3%/2mm and 3%/3mm Gamma criteria with a 10% low dose threshold (LDT) using the SNC Patient software* Version 8.5.1.9 (Sun Nuclear Co., FL, USA).

- 1) Static target motion: The phantom was set as it was measured in the PSQA process, as illustrated in Figure 3a. Image-guided radiotherapy (IGRT) was conducted before the measurement. The measurement was performed three times on different dates to evaluate the setup and image registration uncertainty. The total number of measurements for the static target motion was 21.
- 2) **Moving target motion:** The additional equipment was prepared for the target motion measurement. The IC was attached to the 1-dimensional dynamic platform (Model 008PL, CIRS*, VA, USA) as the tracking marker, as demonstrated in Figure 3b. After the image registration, six radiography angles were set at 0°, 60°, 120°, 180°, 240° and 300° for the respiratory cycle prediction. The value of partial difference (PD) was set at 3 per recommendation. The measurement was performed in 8 waveforms for each PSQA plan. The total number of measurements of moving target motion was 56. This number was calculated according to Naing et al. 25

Data and statistical correlation analysis

The surrounding dose was measured at the detector point of the phantom. This detector position was embedded in the phantom at a depth of 29 mm (equivalent to a depth of 33 mm in water). The

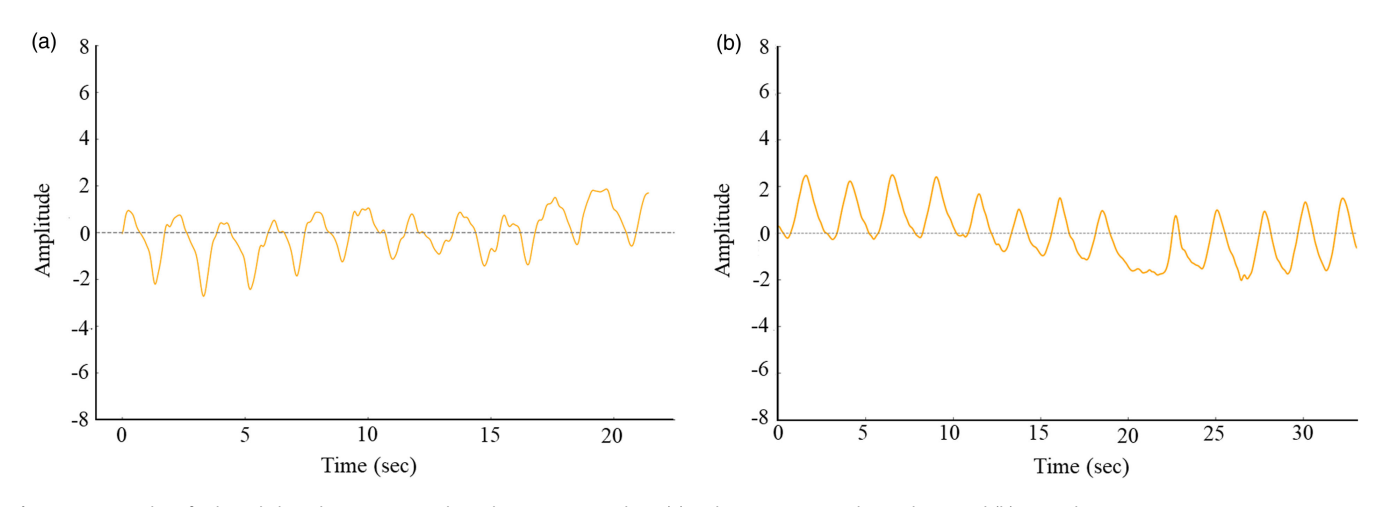


Figure 2. Examples of selected clinical respiratory cycle in the experiment where (a) is the respiratory cycle number 1 and (b) is number 3.

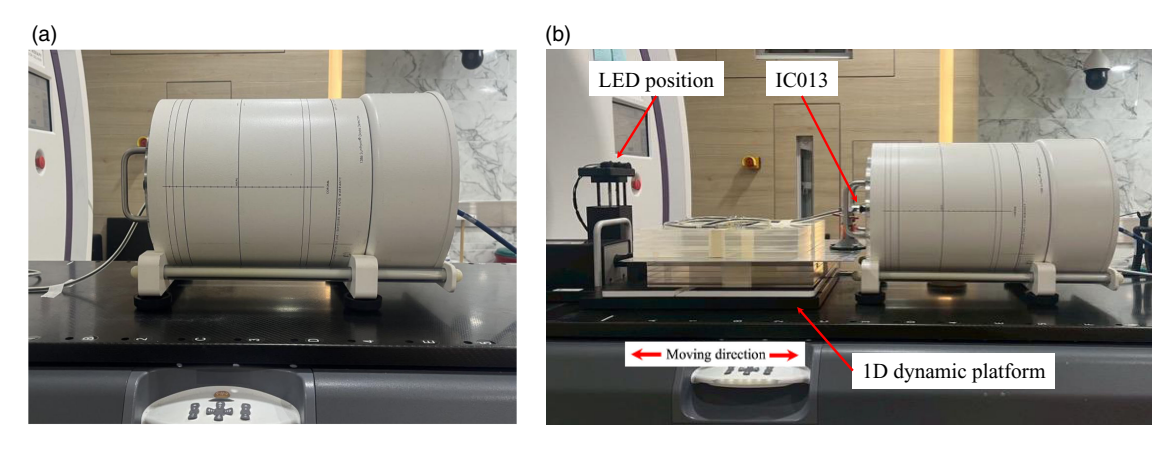


Figure 3. Measurement setup geometry. (a) Static target motion setup and (b) Moving target motion setup.

Table 1. Gamma passing rate value for static and moving target motion

	Static tar	get motion	Moving target motion					
Plan	GPR _{3%/2mm} (%)	GPR _{3%/3mm} (%)	GPR _{3%/2mm} (%)	GPR _{3%/3mm} (%)				
1	99·7 ± 0.0	100·0 ± 0·0	79·2 ± 21·8	84·6 ± 20·5				
2	99·5 ± 0·1	99·7 ± 0·1	85·3 ± 11·3	90·1 ± 10·2				
3	96·1 ± 0·9	98·6 ± 0·3	86·6 ± 9·1	93·8 ± 7·0				
4	97·3 ± 3·9	100·0 ± 0v0	96·8 ± 3·5	99·0 ± 1·4				
5	98·4 ± 1·1	99·7 ± 0·1	97·7 ± 1·0	99·4 ± 0·7				
6	97·0 ± 2·7	99·7 ± 0·5	86·3 ± 9·7	92·6 ± 6·4				
7	97·0 ± 2·7	99·4 ± 0·4	95·3 ± 6·9	97·0 ± 5·5				
Mean ± SD	97·8 ± 1·9	99·5 ± 0·6	90·6 ± 11·7	94·5 ± 9·8				

DD between static target motion and moving target motion was evaluated through point-to-point analysis and expressed as a frequency of percentage level. This frequency of percentage DD was then analysed in correlation with the respiratory frequency, size of planning target volume and target travelling distance. The Shapiro-Wilk test was used to analyse the data distribution. The Pearson correlation coefficient was used for data with normal

distribution, whereas the Spearman correlation coefficient was used for data with non-normal distribution. The statistical correlation was evaluated using SPSS version 27 (IBM Co., NY, USA) with a 95% confidence interval (p-value < 0.05).

Results

The study revealed the characteristic data in the size of PTV, respiratory frequency and target travelling distance. Mean PTV size was 19.6 ± 10.6 cm³ (6.2 cm³– 32.5 cm³) with the width, length and height measuring 29.0 ± 8.6 mm, 32.0 ± 10.6 mm and 35.5 ± 14.8 mm, respectively. The average respiratory frequency and target travelling distance were 24.4 ± 6.0 cycles/min (15.8 cycles/min – 32.8 cycles/min) and 8.3 ± 3.2 mm (5.1 mm – 13.3 mm), respectively.

Gamma passing rate value of static and moving target motion

The GPR value expressed the delivery quality when compared to the dose calculation. The GPR value was revealed in Table 1. Mean GPR values of 3%/2mm and 3%/3mm were $97.8 \pm 1.9\%$ and $99.5 \pm 0.6\%$, respectively, for a static target motion. On the other hand, the GPR of a moving target motion was measured when the target had a motion and the radiation beam was tracking the target location. The mean GPR value then was decreased to $90.6 \pm 11.7\%$ and $94.5 \pm 9.8\%$ for a sequence of Gamma criteria, respectively, as well.

	Frequency of percent dose difference (%)													
Plan	0%-1%	1%-2%	2%-3%	3%-4%	4%-5%	5%-10%	10%-15%	15%-20%	20%-25%	25%-30%	> 30%			
1	17·7 ± 0·1	8·4 ± 4·4	7·9 ± 3·5	7·.0 ± 3·2	6·0 ± 2·4	19·5 ± 3·6	7·7 ± 2·1	5·1 ± 2·2	4·1 ± 2·1	2·8 ± 2·6	13·8 ± 15·9			
2	18·6 ± 7·5	10·0 ± 3·1	9·1 ± 2·1	7·5 ± 1·2	7·2 ± 1·4	22·2 ± 7·4	8·7 ± 4·3	3·5 ± 1·8	2·9 ± 2·3	2·2 ± 2·0	8·1 ± 5·4			
3	17·8 ± 2·9	8·3 ± 1·5	7·2 ± 1·4	7·3 ± 1·1	6·5 ± 1·6	23·4 ± 3·1	11·7 ± 3·1	6·1 ± 1·5	4·1 ± 1·6	2·8 ± 1·5	4·7 ± 4·3			
4	14·3 ± 6·4	7·3 ± 4·2	6·3 ± 2·6	6·2 ± 2·5	5·8 ± 1·4	19·5 ± 3·7	11·5 ± 3·3	7·3 ± 2·3	5·2 ± 2·8	3·2 ± 2·5	13·3 ± 12·1			
5	20·7 ± 2·3	10·8 ± 2·5	10·5 ± 1·7	9·1 ± 1·3	6·7 ± 0·8	16·1 ± 2·0	8·0 ± 1·9	3·5 ± 0·6	3·0 ± 1·8	3.8 ± 2.2	7·8 ± 4·1			
6	9·7 ± 2·4	4·9 ± 1·4	4.6 ± 1.8	3·8 ± 2·0	5·1 ± 1·8	18·7 ± 4·6	11·9 ± 4·2	7·4 ± 3·3	6·5 ± 1·8	5·3 ± 1·7	22·0 ± 14·9			
7	16·1 ± 4·4	7·5 ± 3·4	7·5 ± 3·9	6·2 ± 3·1	5·3 ± 2·1	19·5 ± 4·0	13·8 ± 4·9	8·6 ± 4·7	6·6 ± 4·1	3.6 ± 4.0	5·4 ± 10·2			
Mean ± SD	16·4 ± 6·5	8·2 ± 3·5	7·6 ± 3·1	6·7 ± 2·6	6·1 ± 1·8	19·8 ± 4·7	10·5 ± 4·0	5·9 ± 3·1	4.6 ± 2.7	3·4 ± 2·5	10·7 ± 11·5			

Table 2. Frequency of different levels of percent dose difference at point-to-point between static and moving target motion

(a)	a)										_ (b)												
	-325	320	-315	-310	-305	-300	-295	-290	-285	-280	-275	-2 F		-325	324	-323	-322	-321	-320	-319	-318	-317	-316	-315
48	12-1744		12-4325		12-0921		12-1666		12-5655		12-1372		48	10.7644	0.7739	10-7811	10.7833	10-7621	10.7457	10-7224	10-6876	10-6603	10-6333	10-6082
13													17	11-0610	11.0675	11-0731	11-0735	11-0514	11-0362	11-0161	10-9849	10.9660	10-9469	10-9235
38	15-7263		15-5964		15.9037		15.7969		15-6530		15-9394	- 1	46	11-3680	11-3717	11-3820	11-3861	11-3640	11-3464	11-3262	11-2978	11-2821	11-2673	11-2494
33	71-8973		74 6005		72 5402		75.0054		76.0407		CE EC30	- 1	45	11-6741	11-6761	11-6915	11-6998	11-6781	11-6583	11-6379	11-6125	11-5997	11-5888	11-5771
28	/1-89/3		71-6025		72-5182		75-8251		76-9487		65-5639	- 1	14	11-9803	11-9805	12-0009	12-0135	11-9922	11-9701	11-9496	11-9272	11-9173	11.9103	11-9049
10	127-3064		131-6936		134-1190		142-3960		151-4371		147-5924	- 1	43	12-3206	12-3279	12-3505	12-3620	12-3379	12-3157	12-2985	12-2770	12-2612	12-2513	12-2523
13	127-3004		131-0930		134-1190		142-3900		131.43/1		147-3924	- 1	1 2	12-6609	12-6760	12-7014	12-7121	12-6856	12-6640	12-6512	12-6310	12-6087	12-5954	12-6032
8	124-8152		135-1075		134-1061		141-6860		151-7090		153-1107	- [41	13-0012	13-0241	13-0522	13-0622	13-0333	13-0124	13-0039	12-9849	12-9562	12-9395	12-9540
3	12.0102		100 1070				1.1. 0000		101 / 000		100 1107		40	13-4481	13-4648	13-4915	13-4983	13-4641	13-4400	13-4290	13-4128	13-3924	13-3799	13-3947
-2	112-2944		126 · 1472		128-6141		128-4369		131-3748		136-2568		39	13-8950	13-9070	13-9335	13-9384	13-9003	13-8741	13-8613	13-8495	13-8409	13-8356	13-8514
-7													38	14-3419	14-3492	14-3755	14-3786	14-3365	14-3083	14-2935	14-2861	14-2894	14-2913	14-3082
-12	78-9812		89-4377		93-2511		90-9349		87-2039		89-0233		37	15-0920	15-1052	15-1363	15-1409	15-0913	15-0418	15-0059	14-9853	14-9862	14-9905	15-0101
-17												I 16	36	15-8421	15-8660	15-9070	15-9185	15-8667	15-8000	15-7463	15-7155	15-7173	15-7282	15-7557
			_		_		_			_			35	16-5922	16-6267	16-6777	16-6962	16-6421	16-5581	16-4867	16-4458	16-4484	16-4658	16-5014

Figure 4. Point-to-point dose comparison where (a) Measured dose point and (b) Calculated dose point. Number of yellow highlight is the dose at the detector position.

Dose difference in the surrounding area evaluation

The dose distribution was compared between the static and moving target motion. According to the detector position, the percent DD was calculated using point-to-point comparison, as illustrated in Figure 4. These DD values were classified into the frequency of the percent DD level. The results of the analysis were described in Table 2 and demonstrated in Figure 5. The frequency showed the highest value at the percent DD level of 5-10%, with the second and third highest values revealed in 0-1% and more than 30% levels, respectively. Another level of DD frequency value that was considered was 10-15%.

Correlation between the frequency of percent dose difference levels and other target characteristics

This experiment explored the correlation between the surrounding dose area and other target characteristics such as the target travelling distance, PTV size and respiratory frequency. This would demonstrate the influence of target characteristics that impact the area of surrounding dose. The results of the statistical analysis are described in Table 3.

- 1) Target travelling distance correlation: Statistical analysis revealed a significant negative correlation (p = 0.024, r = -0.302) for the frequency of 2 3% DD levels, while the 10 15% DD level revealed a significant positive correlation (p = 0.006, r = 0.363). The bold lines in Figure 6a demonstrate the trend of the data, which show a significant correlation with the frequency of percent dose at different levels.
- 2) **PTV size correlation:** The results showed a significant positive correlation ($p \le 0.005$, $r \ge 0.374$) for the frequency

- of DD levels at 0% 5% as illustrated in Figure 6b. On the other hand, a significant negative correlation (p ≤ 0.002 , r ≤ -0.406) appeared in the frequency of DD levels at 10 25%. A significant correlation of the PTV size was demonstrated by the bold lines in Figure 6b.
- 3) Respiratory frequency correlation: Statistical analysis found no significant correlation between the respiratory frequency and all levels of DD frequency. The p-value was reported to be larger than 0·370, indicating both positive and negative correlations. There are no bold lines in Figure 6c, which was no significant correlation between the frequency of percent DD and respiratory frequency.

Discussion

This study investigated the DD in the surrounding area using the ArcCHECK® phantom. The DD was presented as a frequency of percent DD levels using a point-to-point comparison. Although the IC was used as the tracking marker, the irradiated area did not involve any part of the IC. Sequentially, the DD was evaluated.

Gamma passing rate value of static and moving target motion

This experiment was conducted to confirm the treatment quality using GPR.^{3,26,27} The GPR values clearly demonstrated no limitations of the treatment plan, particularly in static target motion. According to the recommendations of the AAPM Task Group 148²⁸ and Task Group 306,²⁹ the GPR revealed superb values to ensure the performance of the treatment machine for Gamma criteria of 3%/3mm. Although the tighter Gamma criteria (3%/2mm) were employed, the GPR values were above

Table 3. Frequency of different levels of percent dose difference at point-to-point between static and moving target motion

	Frequency of percent dose difference (%)													
Plan	0%-1%	1%-2%	2%-3%	3%-4%	4%-5%	5%-10%	10%-15%	15%-20%	20%-25%	25%-30%	> 30%			
A) Target travelling distance and frequency of percent dose difference correlation														
p-value	0.223	0.128	0.024	0.077	0.149	0.962	0.006	0.185	0.212	0.120	0.143			
r-value	-0.165	-0.206	-0.302	-0.238	-0.195	-0.007	0.363	0.180	0.169	0.210	0.198			
B) PTV size	B) PTV size and frequency of percent dose difference correlation													
p-value	alue 0.003 0.002 0.003 0.001 0.005 0.080 0.002 0.002 0.001 0.086									0786				
r-value	0.396	0.408	0.385	0.431	0.374	0.236	-0.410	-0.406	-0.421	-0.232	-0.037			
C) Respira	C) Respiratory frequency and frequency of percent dose difference correlation													
p-value	0.632	0.550	0.845	0.608	0.812	0.370	0.481	0.316	0.756	0.948	0.947			
r-value	0.065	0.082	0.027	0.070	-0.032	-0.122	-0.096	-0.136	-0.042	0.009	0.009			

Bold letters are a significant correlation.

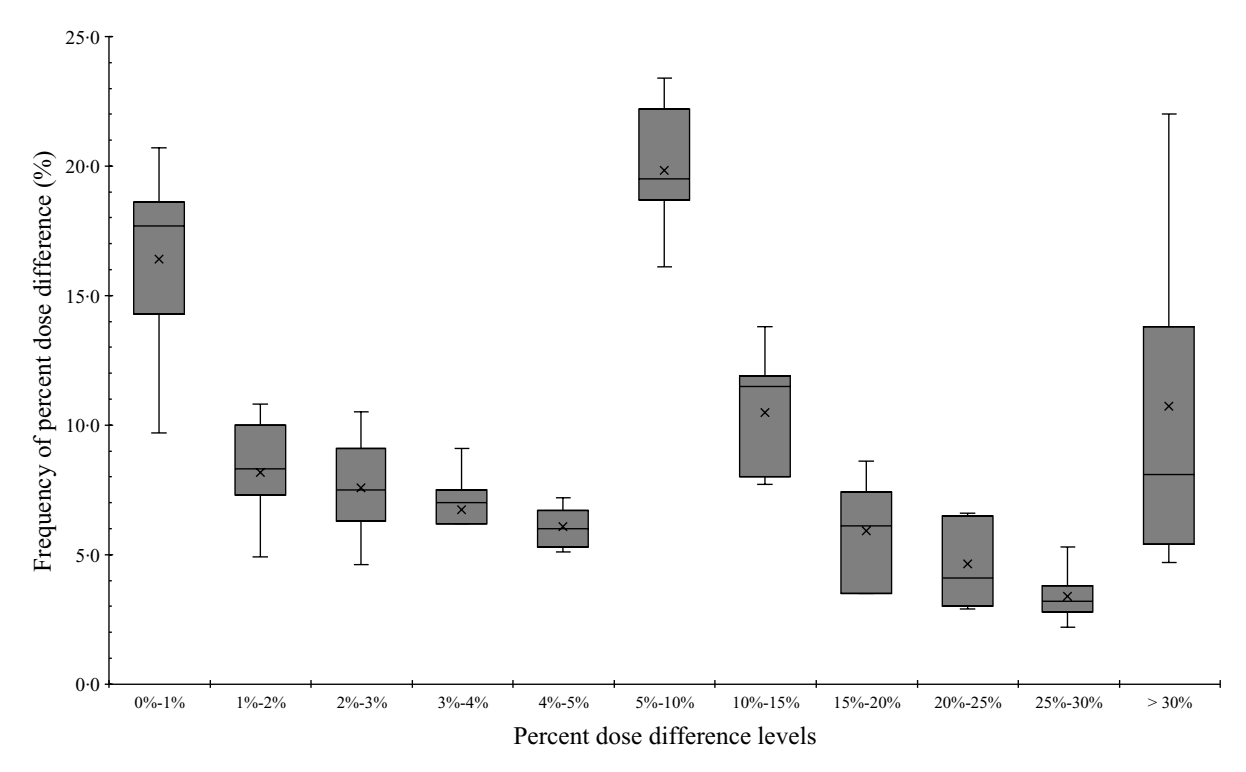
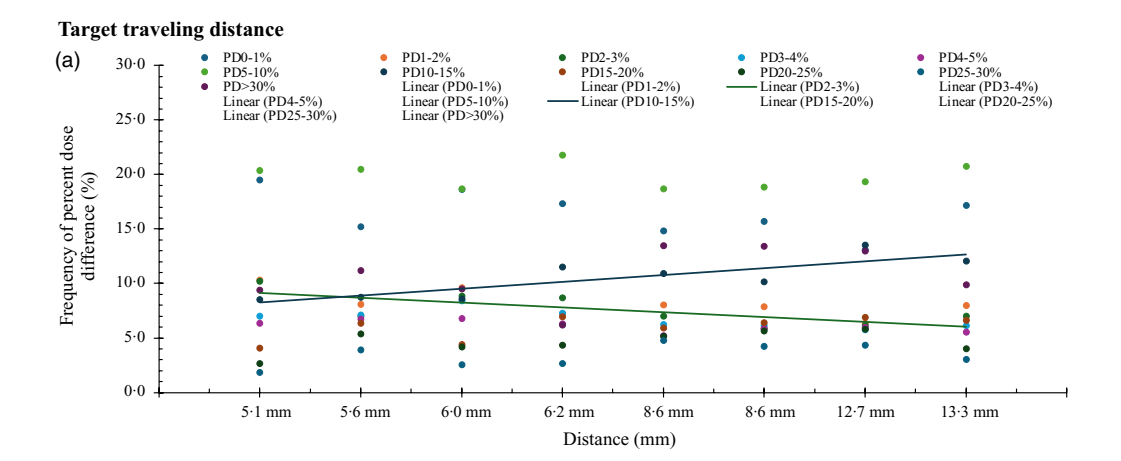


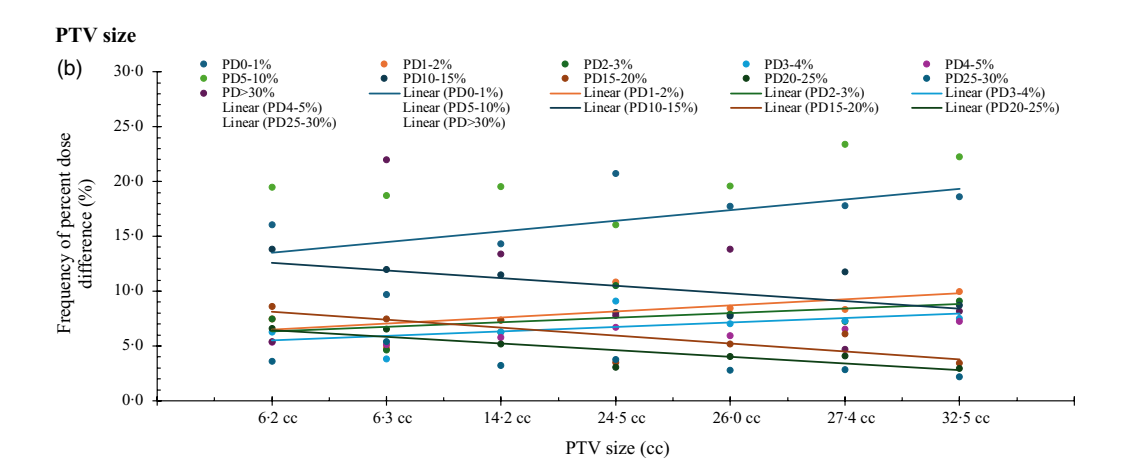
Figure 5. Frequency of percent dose difference separated by percent dose difference levels.

95% as recommended.²⁹ The experiment indicated the low uncertainty in the equipment setup with the standard deviation values within 1.9%. Ensuring that setup uncertainty had minimal influence on the measurement values. In addition, the GPR values revealed a reduction in moving target motion. These measurements were conducted in a target with motion where the radiation mimicked static motion. The results revealed variation values of 11.7% and 9.8% for GPR_{3%/3mm} and GPR_{3%/3mm} respectively. This variation is likely caused by the respiratory frequency and the target travelling distance. This clearly demonstrates the low coverage of radiation dose when static motion delivery is employed on the moving target. Although the GPR_{3%/3mm} value was within an acceptable level, the GPR_{3%/2mm} was at the action level.²⁹

Dose difference in the surrounding area evaluation

The motion of the target during the treatment introduced dose blurring to the target, resulting in the edge of the target receiving the unsharp radiation dose. 12,30 In contrast, the motion management of RTMT^{10,14,31} adapted the radiation beam to follow the target while the peripheral organs remained stationary. The blurring dose would appear on the OARs rather than the target. When considering in Figure 5, the frequency of percent DD revealed high values for DDs below 5%. However, this DD range was not significant due to the recommendations of the International Commission on Radiation Units Measurements (ICRU) number 62 and number 83.32,33 The percent DD levels above 5% were of interest. High values of





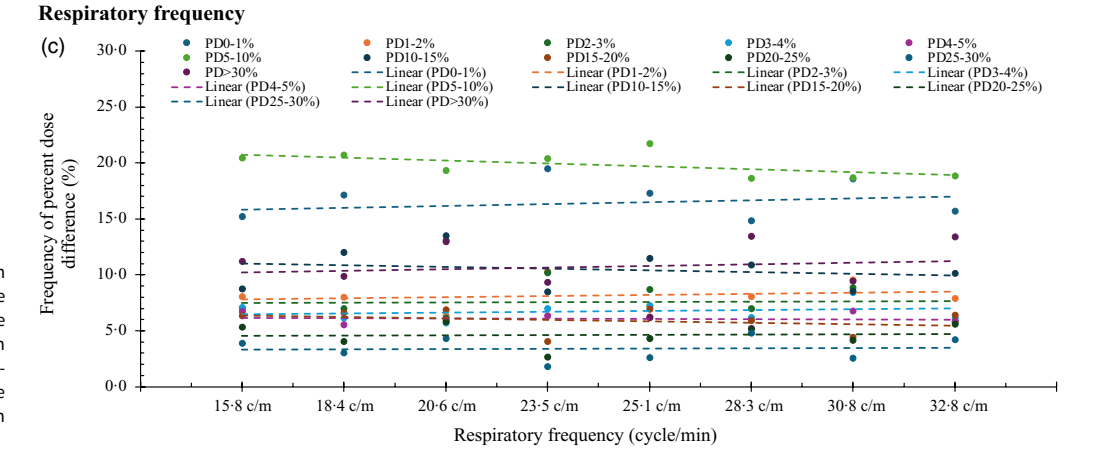


Figure 6. Plots and trend line between the frequency of percent dose difference levels and target characteristics where bold lines are a significant correlation and dash lines are no significant correlation. (a) Target travelling distance correlation, (b) PTV size correlation and (c) Respiratory frequency.

frequency were found at percent difference levels of 5-10% and 10-15%. These values were at the edge of the target's travel path when plotted on the 2-dimensional dose distributions as demonstrated by the blue dots in Figure 7. This clearly indicates that dose blurring had occurred at the distal distance of the target travelling in both superior and inferior directions. This finding aligns with the work of Ferris et al., ¹⁵ where they found at least a 7.6% DD at a 20.0 mm depth from the skin. However, this study had limitations in measuring dose in other surrounding dose

areas due to the specific detector position. The DD was reported at a 33·0 mm water-equivalent depth from the phantom surface. This geometry would be relevant when the target is in the peripheral lung, where the spinal cord remains motionless. In addition, the percent DD showed a high value exceeding 15%. This area can be observed outside the treatment volume, as indicated by the green dots in Figure 7. This demonstrates that the maximum percent DD should be within 15% at this surrounding location.

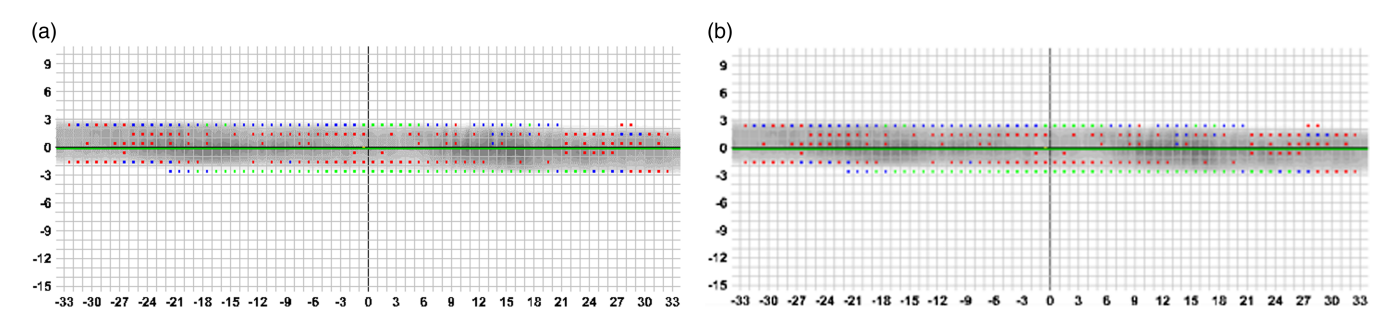


Figure 7. Examples of two-dimensional dose distribution from ArcCHECK® where (a) Dose distribution of treatment planning number 1 and (b) Dose distribution of treatment planning number 2. Colour dots are the positions that had a dose difference at levels of 0 – 5% (red dots), 5 – 15% (blue dots) and more than 15% (green dots).

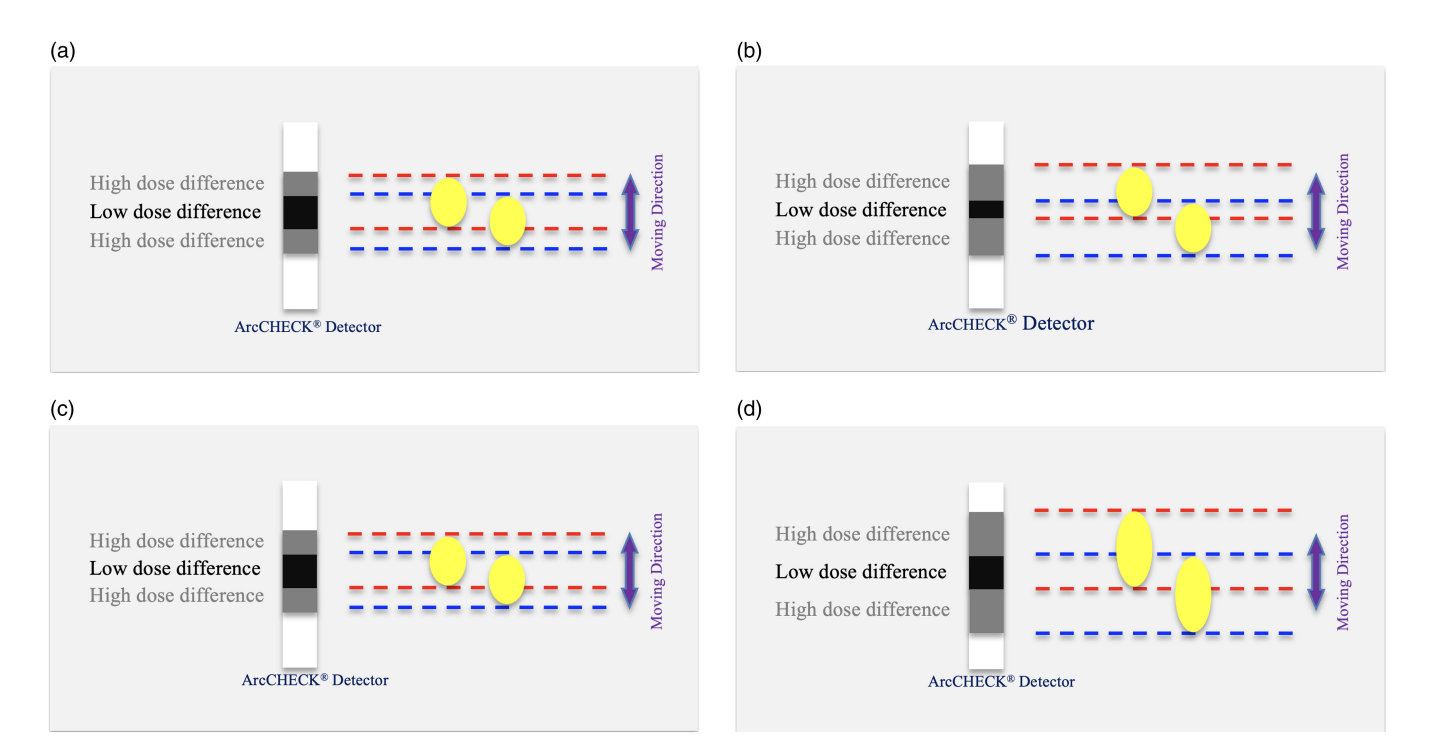


Figure 8. Diagrams of target characteristics impact the frequency of percent dose difference. Upper row demonstrates the area of detector that has a short target travelling distance (a) and a long target travelling distance (b). Bottom row illustrates the area of detector that has a small PTV size (c) and a large PTV size (d).

Correlation between the frequency of percent dose difference levels and other target characteristics

The study investigated the factors of target characteristics that impact the surrounding dose area using RTMT. The correlation focused on major factors such as the target travelling distance, PTV size and respiratory frequency.

1) Target travelling distance correlation: The statistical analysis found a negative correlation between the frequencies of DDs at 2 – 3%, whereas a positive correlation was found at higher DD levels. This may demonstrate the distance of the target impact to the area of the surrounding dose. In short distances, the motion would be much similar to the stationary condition. However, a negative correlation was observed between the DD and the travelling distance. Specifically, at low dose levels, a short travelling distance may increase dose accumulation at the same detector location, thus introducing dose variation. The frequency of DDs was then revealed at the central area of the target

- motion, as illustrated in Figure 8a. In contrast, the area of high DD increased when the target had a long travelling distance, as shown in Figure 8b. This reason then correlated with a significant positive analysis when the distance was increased. This finding confirms the work of Ferris et al. that DDs could occur most frequently in the superior-inferior direction of the target. ¹⁵
- 2) **PTV size correlation:** The PTV size is one factor that impacts the area of the surrounding dose. The analysis found a significant positive correlation when the RTMT was used in a small lesion, whereas a significant negative correlation was found in the large lesion. According to the same travelling distance, the large PTV may provide a large area of high DD as illustrated in Figure 8d, while the small area of high DD is revealed when employed in a small PTV as demonstrated in Figure 8c.
- Respiratory frequency correlation: Although some trend lines revealed a gradient when the respiratory frequency was increased, the statistical analysis did not show a significant

correlation between these two parameters. The respiratory frequency then may not be a factor that impacts the surrounding dose area.

Although this study investigated the DD in the surrounding area, some limitations were identified. The investigated dose was measured in a phantom with a specific detector position, leading to specific positions of observation for the surrounding dose area, particularly in point-to-point observations. Investigating DDs in volume could be an area of interest for future research. Another limitation was that the location of the lesion was translated to the centre of the phantom, which may not be applicable in clinical practice. However, the geometry could still be represented in the relationship between the peripheral lung lesion and the spinal cord. Another issue was raised regarding in the direction between the respiratory cycle and platform motion. Due to the single direction of the platform model, the vertical respiratory direction from the SentinelTM was converted to the longitudinal platform direction. While this may not accurately reflect the clinical situation, the signals were derived from clinical practice. This could be another interesting issue for further study, potentially utilizing a threedimensional platform. A final limitation of this study was the small number of clinical cases (n = 7). Although the total sample size was increased by including multiple respiratory cycles, the study was restricted to only seven cases due to the short period of RTMT implementation. This limitation presents an opportunity for further investigation.

Conclusion

A RTMT system can deliver the radiation dose using target tracking. During radiation beam tracking the target, a difference between the calculated radiation dose and the measured radiation dose was observed. The DD at a distance of 105 mm from the phantom's centre (119·5 mm water-equivalent distance) showed a maximum frequency at a DD of 5 – 10% using point-to-point measurement. However, the DD could be as high as 10 – 15% if the target had a long distance to travel and a larger size of target. This was confirmed by the significant correlation between the DDs and the distance of the target travelling and the size of the PTV, whereas no significant correlation was found with the respiratory frequency.

Acknowledgements. No acknowledgment for this study.

Author's contributions. (1) Phairot Kititharakun: Conceptualization, Data curation, Investigation, Formal analysis, Writing – original draft, Writing – review and editing.

- (2) Wannapha Nobnop: Formal analysis, Writing review and editing.
- (3) Anupong Kongsa: Formal analysis.
- (4) Warit Thongsuk: Formal analysis.
- (5) Anirut Watcharawipha: Conceptualization, Formal analysis, Writing review and editing, Supervision.

Financial support. The authors declare that no funds, grants, or other support were received on this study.

Competing interests. This study has no conflict of interest.

Presentation at a conference. Oral presentation at the 23rd South-East Asia Congress of Medical Physics (SEACOMP) – 16th Annual Meeting of Thai Medical Physicist Society (TMPS), Chiang Rai, Thailand.

Ethics. This study protocol was approved by the Research Ethics Committee of Faculty of Medicine, Chiang Mai University (Study code: RAD-2567-0221).

References

- Yenice KM, Narayana A, Ghang J, Gutin PH, Amols HI. Intensity modulated stereotactic radiotherapy (IMSRT) for skull-base meningiomas. Int J Radiat Oncol Biol Phys 2006; 66 (4): S95–S101. doi: 10.1016/j.ijrobp. 2005.09.040
- Oh SA, Kang MK, Kim SK, Yea JW. Comparison of IMRT and VMAT Techniques in Spine Stereotactic Radiosurgery with International Spine Radiosurgery Consortium Consensus Guidelines. Prog Med Phys 2013; 24 (3): 145–153. doi: 10.14316/pmp.2013.24.3.145
- Chaiyapong A, Watcharawipha A, Nobnop W, Kongsa A, Jia-Mahasap B. Feasibility of large multi-leaf collimator in stereotactic radiosurgery/ stereotactic radiotherapy: a single center experience. Biomed Sci Clin Med 2025; 64 (1): 35–45. doi: 10.12982/BSCM.2025.02
- Watcharawipha A, Chakrabandhu S, Kongsa A, Tippanya D, Chitapanarux I. Plan quality analysis of stereotactic ablative body radiotherapy treatment planning in liver tumor. J Appl Clin Med Phys 2023; 24: e13948. doi: 10. 1002/acm2.13948
- Watcharawipha A, Chitapanarux I, Jia-Mahasap B. Dosimetric comparison of large field widths in helical tomotherapy for intracranial stereotactic radiosurgery. Inter J Radiat Res 2022; 20 (3): 701–707. doi: 10.52547/ijrr.20. 3.26
- Saw CB, Gillette C, Peters CA, Koutcher L. Clinical implementation of radiosurgery using helical tomotherapy unit. Med Dosim 2018; 43: 284– 290. doi: 10.1016/j.meddos.2017.10.004
- Manabe Y, Murai T, Ogino H, et al. CyberKnife stereotactic radiosurgery and hypofractionated stereotactic radiotherapy as first-line treatments for imaging-diagnosed intracranial meningiomas. Neurol Med Chir (Tokyo) 2017; 57 (12): 627–633. doi: 10.2176/nmc.oa.2017-0115
- Ding C, Saw CB, Timmerman RD. Cyberknife stereotactic radiosurgery and radiation therapy treatment planning system. Med Dosim 2018; 43 (2): 129–140. doi: 10.1016/j.meddos.2018.02.006
- Tawfik ZA, Farid ME, El Shahat KM, Hussein AA, Eldib AA, Etreby MA. A
 dosimetric study comparing Cyberknife and LINAC-based stereotactic
 radiotherapy or radiosurgery treatments. J Radiat Res Appl Sci 2024; 17 (1):
 100781. doi: 10.1016/j.jrras.2023.100781
- American Association of Physicists in Medicine. The management of respiratory motion in radiation oncology: Report No.91. Maryland, United states of America; 2006.
- 11. Sumida I, Shiomi H, Higashinaka N, et al. Evaluation of tracking accuracy of the CyberKnife system using a webcam and printed calibrated grid. J Appl Clin Med Phys 2016; 17 (2): 74–84. Published 2016 Mar 8. doi: 10. 1120/jacmp.v17i2.5914
- Ferris WS, Kissick MW, Bayouth JE, Culberson WS, Smilowitz JB. Evaluation of radixact motion synchrony for 3D respiratory motion: modeling accuracy and dosimetric fidelity. J Appl Clin Med Phys 2023; 24 (1): e13805.
- Schnarr E, Beneke M, Casey D, et al. Feasibility of real-time motion management with helical tomotherapy. Med Phys 2018; 45 (4): 1329–1337. doi: 10.1002/mp.12791
- Dhont J, Harden SV, Chee LYS, Aitken K, Hanna GG, Bertholet J. Imageguided radiotherapy to manage respiratory motion: lund and liver. Clin Oncol 2020; 32: 792–804. doi: 10.1016/j.clon.2020.09.008
- Ferris WS, Chao EH, Smilowitz JB, Kimple RJ, Bayouth JE, Culberson WS.
 Using 4D dose accumulation to calculate organ-at-risk dose deviations
 from motion-synchronized liver and lung tomotherapy treatments. J Appl
 Clin Med Phys 2022; 23 (7): e13627.
- Niroomand-Rad A, Blackwell CR, Coursey BM, et al. Radiochromic film dosimetry: recommendations of AAPM radiation therapy committee task group 55. Med Phys 1998; 25 (11): 2093–2115. doi: 10.1118/1.598407
- Casanova Borca V, Pasquino M, Russo G, et al. Dosimetric characterization and use of GAFCHROMIC EBT3 film for IMRT dose verification. J Appl Clin Med Phys 2013; 14 (2): 158–171.
- Bouchard H, Lacroix F, Beaudoin G, Carrier JF, Kawrakow I. On the characterization and uncertainty analysis of radiochromic film dosimetry. Med Phys 2009; 36 (6): 1931–1946. doi: 10.1118/1.3121488
- 19. Akdeniz Y. Comparative analysis of dosimetric uncertainty using Gafchromic™ EBT4 and EBT3 films in radiochromic film dosimetry.

- Radiat Phys Chem 2024; 218: 111723. doi: 10.1016/j.radphyschem.2024. 111723.
- Buonamici FB, Compagnucci A, Marrazzo L, Russo S, Bucciolini M. An intercomparison between film dosimetry and diode matrix for IMRT quality assurance. Med Phys 2007; 34 (4): 1372–1379. doi: 10.1118/1.2713426
- Son J, Baek T, Lee B, et al. A comparison of the quality assurance of four dosimetric tools for intensity modulated radiation therapy. Radiol Oncol 2015; 49 (3): 307–313. Published 2015 Aug 21. doi: 10.1515/raon-2015-0021
- Létourneau D, Gulam M, Yan D, Oldham M, Wong JW. Evaluation of a 2D diode array for IMRT quality assurance. Radiother Oncol 2004; 70 (2): 199–206. doi: 10.1016/j.radonc.2003.10.014
- Accuray Incorporated. Clinical checklist for Synchrony® on the Radixact® System: DOC-00235.A. California, The United States of America; 2024.
- Sano K, Fujiwara M, Okada W, Tanooka M, Takaki H, Shibata M, et al. Optimal threshold of a control parameter for tomotherapy respiratory tracking: a phantom study. J Appl Clin Med Phys 2023; 24: e13901. doi: 10. 1002/acm2.13901
- Naing L, Winn T, Rusli B. Practical issues in calculating the sample size for prevalence studies. Archives of orofacial Sciences 2006; 1: 9–14.
- Watcharawipha A, Chitapanarux I. Gamma analysis of patient specific quality assurance by hybrid acceptance criterion method. Inter J Radiat Res 2023; 21 (3): 505–512. doi: 10.52547/ijrr.21.3.21

- Saengsawatdiphong T, Watcharawipha A, Nobnop W. Evaluation of tolerance and action limits for delivery quality assurance in two tomotherapy platforms based on AAPM TG-218 recommendations. Health Technol 2025. doi: 10.1007/s12553-025-00962-y
- Langen KM, Papanikolaou N, Balog J, et al. QA for helical tomotherapy: report of the AAPM task group 148. Med Phys 2010; 37: 4817–4853. doi: 10. 1118/1.3462971
- Chen Q, Rong Y, Burmeister JW, et al. AAPM task group report 306: quality control and assurance for tomotherapy: an update to task group report 148.
 Med Phys 2023; 50 (3): e25-e52. doi: 10.1002/mp.16150
- Bortfeld T, Jiang SB, Rietzel E. Effects of motion on the total dose distribution. Semin Radiat Oncol 2004;14 (1):41–51.
- Keall PJ, Mageras GS, Balter JM, et al. The management of respiratory motion in radiation oncology report of AAPM Task Group 76. Med Phys 2006; 33 (10): 3874–3900. doi: 10.1118/1.2349696
- International Commission of Radiation Units and measurements. ICRU Report 62 — Prescribing, Recording and Reporting Photon Beam Therapy (Supplement to ICRU Report 50). Report No 62. Bruxelles, Belgium; 1999.
- International Commission of Radiation Units and measurements. ICRU Report 83 — Prescribing, Recording and Reporting Photon Beam Therapy. Report No 83. Washington DC, The United States of America; 2010.